

## Enhanced Crystallization of Bisphenol-A Polycarbonate by Organoclay in the Presence of Sulfonated Polystyrene Ionomers

Patakamuri Govindaiah, Jung Min Lee, Seung Mo Lee, and Jung Hyun Kim\*

*Department of Chemical and Biomolecular Engineering, Yonsei University, Seoul-120-749, Korea*

Sankaraiah Subramani

*Department of Chemistry, Missouri University of Science and Technology, Rolla, Missouri-65409-0010*

*Received January 13, 2009; Revised May 11, 2009; Accepted May 12, 2009*

**Abstract:** Polycarbonate (PC)/sulfonated polystyrene (SPS) ionomer/organoclay nanocomposites were prepared by a solution intercalation process using the SPS ionomer as a compatibilizer. The effect of an organoclay on the melt crystallization behavior of the ionomer compatibilized PC were examined by differential scanning calorimetry (DSC). The melt crystallization behavior of PC was dependent on the extent of organoclay dispersion. The effect of the ionomer loading and cation size on intercalation/exfoliation efficiency of the organoclay in PC/SPS ionomer matrix was also studied using wide angle X-ray diffraction (WAXD) and transmission electron microscopy (TEM). Dispersion of the organically modified clay in the polymer matrix improved with increasing ionomer compatibilizer loadings and cation size. The SPS ionomer compatibilized PC/organoclay nanocomposite showed enhanced melt crystallization compared to the SPS ionomer/PC blend. Well dispersed organoclay nanocomposites showed better crystallization than the poorly dispersed clay nanocomposites. These nanocomposites also showed better thermal stability than the SPS ionomer/PC blend.

**Keywords:** nanocomposites, polycarbonate, melt crystallization, sulfonated polystyrene ionomers, compatibilizer.

### Introduction

Polymer/layered silicate nanocomposites have been a great interest to researchers in both academia and industry because of their significant improvement in physical, thermal and barrier properties when compared with virgin polymers, even in very low filler loadings.<sup>1-7</sup> The enhancement in physical properties includes high modulus, increased heat resistance, decreased gas permeability and decreased flammability provided by nanoparticle reinforcement. In addition, molecularly dispersed clay layers also reported to improve the crystallization behavior of matrix polymers. The enhancement in the properties of these materials was due to the interactions between the polymer chains and the surface of clay layers.<sup>8</sup> The property improvement was maximized when the clay layers were completely delaminated or exfoliated in the polymer matrix because of its high aspect ratio.

Bisphenol-A polycarbonate is commonly known as a clear and amorphous thermoplastic when processed from a melt. PC undergoes thermal-induced crystallization very slowly because its chain rigidity retards the chain diffusion. At 190 °C, one full day is necessary to develop the first crys-

tallite and a week or more to obtain a well developed spherulite.<sup>9</sup> PC crystallizes when exposed to solvents<sup>10</sup> or during precipitation; however, it does not crystallize after melting. Weiss *et al.*<sup>11</sup> reported that PC was melt crystallized when blended with polystyrene ionomers. The melt crystallization of PC is a nucleation process nucleated by the nanometer-size ionic aggregated species of SPS ionomer in the PC matrix. Hu *et al.*<sup>12</sup> have shown that, in the presence of CO<sub>2</sub>, nanoscale clay is an efficient nucleating agent that enhances the crystallization of PC. Previous research has shown that the addition of clay into semicrystalline polymers such as syndiotactic polystyrene ionomer,<sup>21</sup> poly(ethylene terephthalate) ionomer<sup>13</sup> and nylon 6<sup>14</sup> can enhance the overall crystallization of the matrix polymer due to the nucleation effect of molecularly dispersed clay layers. The crystallization of the matrix polymer was faster when clay layers were completely exfoliated.<sup>22</sup> In this study, we were interested in studying the effect of dispersed nano-clay on melt crystallization behavior of ionomer compatibilized PC.

PC nanocomposites can offer improved physical properties such as strength, modulus, and scratch resistance without sacrificing optical clarity and toughness. There is limited literature on PC/clay nanocomposites mainly because of the weak interactions between the matrix polymer and the polar

\*Corresponding Author. E-mail: jayhkim@yonsei.ac.kr

layered silicate surface. The unchanged polymer backbone restricts the interactions between the non-ionic polymer and clay surface, even though the clay surface is organophilic.<sup>15</sup> Polymer chain cannot be enter into clay lattice due to weak interactions between non-ionic polymer chain and clay surface. To improve interactions with the clay surface, the polymer chain needed to be modified with ionic groups. Much effort has been focused in improving the dispersion of clay in PC matrix. Huang *et al.*<sup>16</sup> synthesized well-dispersed PC/layered silicate nanocomposites via cyclic oligomerization. Compatibilizing with ionic polymers can also result in exfoliated structures by improving the interactions between the clay layers and the matrix polymer. Recently, researchers obtained exfoliated layers in variety of polymers by compatibilizing them with functionalized ionomers. An example is given by Bhiwabkar *et al.*,<sup>17</sup> who reported that SPS ionomer is an effective compatibilizing agent for mixing of hydrophobic polymers, such as polystyrene, into the clay. Paul *et al.* compared the dispersion efficiency between amine functionalized polypropylene and maleated polypropylene as a compatibilizer in preparing polypropylene nanocomposites.<sup>18</sup> They have also studied the effect of neutralizing cation on the exfoliation efficiency of poly(ethylene-co-methacrylic acid) ionomers/organoclay nanocomposite.<sup>19</sup> Zinc and sodium ionomers show much better exfoliation of organoclay compared to the equivalent nanocomposites prepared from smaller ionomer cations such as a lithium. Park *et al.*<sup>20,21</sup> prepared well dispersed syndiotactic polystyrene (sPS)/organoclay nanocomposites by stepwise melt blending with functionalized atactic polystyrene. Many research efforts were also focused on functionalized ionomer/clay nanocomposites to enhance dispersion of nanolayers in the polymer matrix. Nanocomposites with sulfonated sPS ionomers,<sup>22</sup> sulfonated poly(ethylene terephthalate) ionomers,<sup>23</sup> sulfonated poly(butylene terephthalate) ionomers,<sup>24</sup> end functionalized polypropylene ionomers,<sup>25</sup> polyethylene ionomers,<sup>26</sup> silylated polyurethane-acrylic hybrids<sup>27</sup> and polyethylene/polyethylene ionomer blends<sup>28</sup> also obtained good levels of exfoliation with organoclay. However, in this study we focused on obtaining well dispersed clay nanostructures in the polymer matrix. Well-dispersed nano-clay can significantly enhance the crystallization properties of matrix polymer.<sup>22,23,29</sup>

Ionomers are attractive materials that promote miscibility between a non-ionic polymer and layered silicate. The ionic groups of ionomers may be used to achieve specific interactions which include hydrogen bonding, ion-dipole, acid base interaction or transition metal complexation between the ionic and nonionic species in the ionomer part of the blend. Many researchers have used PS based ionomers to enhance miscibility with various polymers in the blend. Weiss *et al.*<sup>30-35</sup> studied the effect of ionic groups and cation of SPS ionomers on the miscibility with PC,<sup>30,31</sup> polyamide<sup>33,34</sup> and polypeptide.<sup>35</sup> Intermolecular attractive and repulsive interactions within ionomers favor miscibility with other poly-

mers. Eisenberg *et al.*<sup>36-39</sup> prepared miscible blends of styrene-methacrylic acid/poly(alkylene oxide),<sup>36,37</sup> SPS/polyamide<sup>38</sup> and SPS/polyurethane.<sup>39</sup> Kim *et al.*<sup>40</sup> blended sulfonated and nonsulfonated polysulfone for improving the transport properties. The phase behavior of the blends can be tailored by varying the ionomer content or counter ion size.<sup>41</sup> In addition to improve miscibility, the ionomers can also help improve the dispersion of organoclay in the matrix polymer.

The purpose of our present study is to improve the melt crystallization of ionomer compatibilized PC by clay dispersion. In this study, we discussed the preparation of PC/SPS ionomer blend/organoclay nanocomposite by solution intercalation process and studied the effect of nano-clay on thermal behavior of ionomer compatibilized PC. Additionally, the effect of ionomer loading and counter ion type (Li<sup>+</sup>, Na<sup>+</sup>, K<sup>+</sup>, Rb<sup>+</sup> and Zn<sup>2+</sup>) on intercalation/exfoliation efficiency of organically modified clay in the polymer matrix was examined with WAXD and TEM analysis. We also studied the effect of nano-clay dispersion on thermal stability of ionomer compatibilized PC.

## Experimental

**Materials and Reagents.** Polystyrene ( $M_w=45,000$ ), poly(bisphenol A carbonate) ( $M_w=64,000$ ;  $T_g=150$  °C), acetic anhydride, rubidium hydroxide and lithium hydroxide from Aldrich, USA; organoclay [dimethyl bis(hydrogenated-tallow) ammonium montmorillonite with the trade name Cloisite 20A] from Southern Chemicals, USA; and sodium hydroxide, potassium hydroxide, ethylene dichloride, tetrahydrofuran (THF) and methanol from SK Chemicals, South Korea were used as received. SPS ionomers were prepared in our laboratory. Other reagents were analytical reagent grade and were used as received.

**Preparation of SPS Ionomers.** SPS ionomers were prepared in a similar procedure reported elsewhere.<sup>42</sup> In a 1 L round bottom flask, PS (6.5 g) and ethylene dichloride (500 mL) were stirred at 70 °C until the PS dissolved completely. Freshly prepared acetyl sulfate solution was added under vigorous stirring, which continued for 3 h. The amount of acetyl sulfate required was determined by the desired amount of sulfonation. Ethanol (10 mL) was added to arrest the reaction. The polymer was precipitated by pouring the solution into methanol (2 L) and the precipitate was filtered. The product was washed several times with hot distilled water and was dried in a vacuum oven at 60 °C for 24 h. The polymer was redissolved in ethylene dichloride, precipitated in excess methanol and filtered and dried in a vacuum oven at 60 °C for 24 h. The degree of sulfonation was determined to be a 3.0 mole% by nonaqueous titration method.

Sulfonated polystyrene ionomers were prepared by neutralizing with 20% excess methanolic alkali hydroxides (LiOH, NaOH, KOH, RbOH and zinc acetate). The neutralized polymer solution was precipitated in excess methanol,

washed with methanol and dried in vacuum at 60 °C for 24 h.

**Preparation of SPS Ionomer/PC Blends.** SPS ionomer/PC blends were prepared by solution blending. PC solution in THF (4%, w/v) was added drop by drop to the dissolved solution of SPS ionomers in THF/methanol (90/10, v/v). The solution was kept at room temperature for 10 h under constant agitation, and then transferred onto a glass Petri dish. The solvent was allowed to be evaporated at room temperature and the product was dried at 60 °C under vacuum for 24 h.

**Preparation of SPS Ionomer/PC/Organoclay Nanocomposites.** SPS ionomer/PC/organoclay nanocomposites were prepared by solution intercalation method. PC solution in THF (4%, w/v) was added drop-wise to the organoclay dispersed solution of SPS ionomers in THF/methanol (90/10, v/v). The solution was kept at room temperature for 10 h under constant agitation and then transferred into a glass Petri dish. The solvent was allowed to be evaporated at room temperature. The product dried at 60 °C under a vacuum for 24 h. Organoclay content was kept constant (5 wt%) in all the experiments.

**Characterization.** The thermal properties of the samples were analyzed by TA instruments. TGA Q50 was used to determine the thermal stability of the samples as well as the amount of clay present in the nanocomposites. The samples were heated under flowing nitrogen atmosphere from 50 to 800 °C at a heating rate of 10 °C/min and the weight loss was recorded. The crystallization properties were studied using DSC Q10 under standard conditions. The samples were heated under flowing nitrogen from 0 to 250 °C at the rate of 10 °C/min and annealed for 2 min at the end of the cycle to eliminate the prior thermal and solvent history. Then it was rapidly cooled to crystallization temperature (190 °C) and finally annealed for 15 h with 3 h intervals at 190 °C to obtain crystallization. The annealed sample was rapidly cooled to 0 °C and reheated to 250 °C at 10 °C/min to record the melting thermogram. The calorimeter was calibrated using standard protocols. The sample weight was about 4 mg in all experiments.

The WAXD experiments were performed using a Rigaku MiniFlex II diffractometer equipped with a copper target and a diffracted beam monochromator (Cu K $\alpha$  radiation with  $\lambda=1.5406$  Å) with  $2\theta$  scan range of 1.5–30° at room temperature. The specimen of nanocomposites for WAXD was thin film sample melt pressed on a copper block sample holder at 240 °C for a period of 10 sec and then rapidly cooled to room temperature. In order to obtain crystallized films, the amorphous films were annealed at 190 °C for 3 h in an oven under vacuum. Samples for TEM were sectioned using a Drukker Ultra-Microtome with thicknesses of 50–60 nm using a diamond knife at room temperature. Before sectioning for TEM, the samples were heated to 240 °C for a period of 10 to 15 sec and formed into a strand shape specimen that can be conveniently held on the sample holder of the microtoming machine for sectioning. The sections were

collected from water on 300 mesh carbon coated copper grids. TEM imaging was done using a JEM 3010, JEOL electron microscope operating at an accelerating voltage of 300 kV. The density of clay particles was enough to produce contrast between polymer and clay stacks; hence, staining was not required. Images were captured using charged couple detector (CCD) camera for further analysis using Gatan Digital Micrograph analysis software.

## Results and Discussion

PC/SPS ionomer blends and PC/SPS ionomer/organoclay nanocomposites with various ionomer cations were prepared by solution intercalation process. All work described in this paper was done with an incorporation of 5 wt% montmorillonite modified with dimethyl bis(hydrogenated tallow) ammonium cation. Since it was reasonable to study the effect of SPS ionomers in the nanocomposites, we have formulated nanocomposites at a higher clay loading (5 wt%). Before studying the crystallization behavior we studied the extent of clay dispersion with various ionomer amount and cation type. The spacing between clay platelets or gallery spacing is an indication of the extent of intercalation/exfoliation of clay platelets within a polymer matrix. Figures 1–3 describe the effect of ionomer amount and the cation type on dispersion of organoclay in the polymer matrix; the d-spacing values were listed in Table I. Figure 1 shows an X-ray diffraction pattern of pure organoclay and PC/SPS ionomer/organoclay nanocomposites compatibilized with various loadings of H<sup>+</sup>SPS. The WAXD pattern of pure

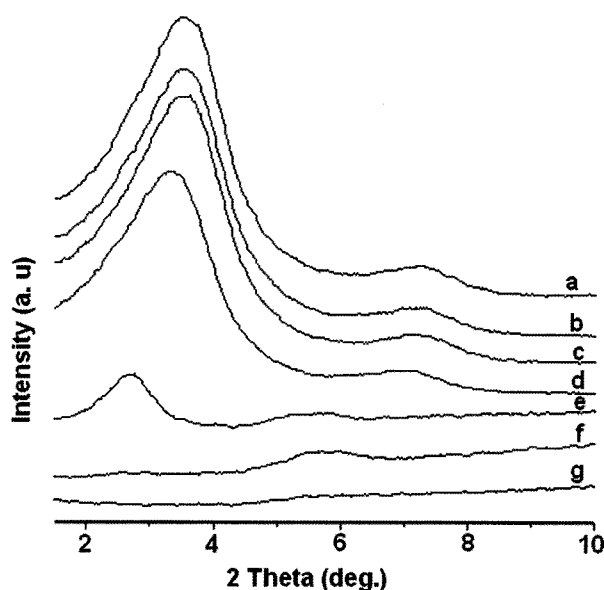


**Figure 1.** XRD pattern of (a) organoclay, (b) PC/organoclay and various ionomer loadings (wt%); (c) 10%, (d) 20%, (e) 30%, (f) 40%, and (g) 50%; in compatibilized PC/H<sup>+</sup>SPS/organoclay nanocomposite.

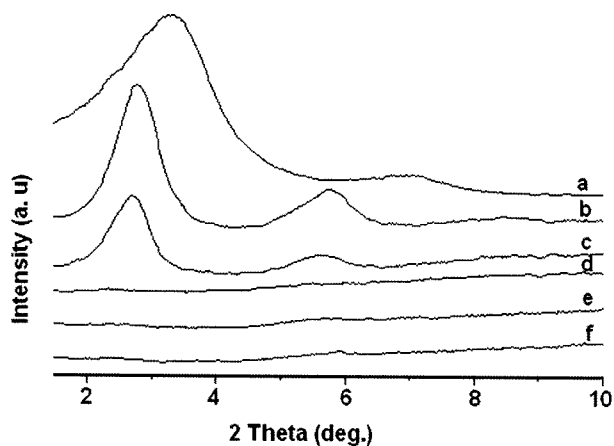


**Figure 2.** XRD pattern of PC/SPS ionomer/organoclay nanocomposite compatibilized with various ionomer cations of SPS (20 wt%): (a) H<sup>+</sup>, (b) Li<sup>+</sup>, (c) Na<sup>+</sup>, (d) K<sup>+</sup>, (e) Rb<sup>+</sup>, and (f) Zn<sup>2+</sup>.

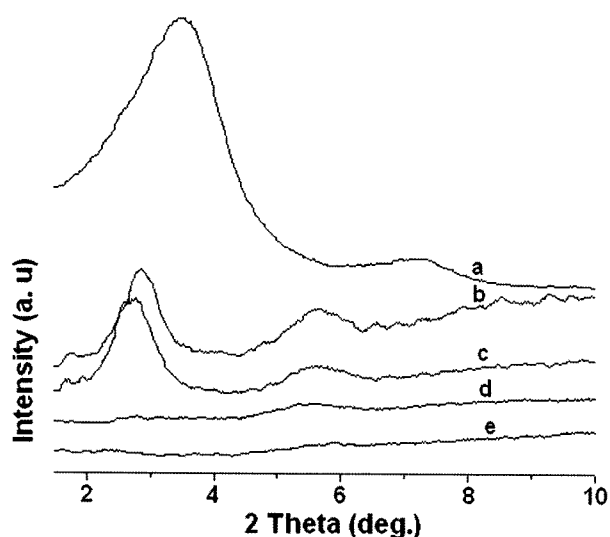


**Figure 3.** XRD pattern of PC/SPS ionomer/organoclay nanocomposite with various ionomer loadings of Zn<sup>2+</sup>SPS: (a) 0%, (b) 5%, (c) 10%, (d) 15%, and (e) 20%.

organoclay shows an intense peak at  $2\theta=3.58^\circ$  with gallery height of around 24.6 Å which is characteristic of the gallery height for modified layered silicate; the peak for PC/organoclay and nanocomposite with 10 wt% H<sup>+</sup>SPS did not show any shift in the position. The position of the peak that corresponds to organoclay did not shift much for the PC/organoclay nanocomposites. Samples prepared with 0 and 10 wt% H<sup>+</sup>SPS loadings showed gallery heights of about 25.1 and 25.2 Å, respectively, indicating no intercalation. The position of the characteristic peak for organoclay in PC/SPS ionomer/organoclay nanocomposites blended with 20 and 30 wt% H<sup>+</sup>SPS was shifted to lower  $2\theta$  and observed at  $2\theta=3.36^\circ$  and  $2.70^\circ$  (gallery heights 26.3 and 36.7 Å, respectively), indicating intercalated structures. Nanocomposites prepared with higher ionomer loadings, i.e. 40 and 50 wt%,

**Table I.** Clay Gallery Height from XRD Data with Various Amount of Ionomer and Cation Type in the Nanocomposites

Composition (wt%)	2 Theta (deg.)	Clay Gallery Height (Å)
H <sup>+</sup> SPS/PC/Organoclay		
Pure Organoclay	3.58	24.6
0/95/5	3.51	25.1
10/85/5	3.50	25.2
20/75/5	3.36	26.3
30/65/5	2.70	32.7
40/55/5	*	*
50/45/5	*	*
SPS Ionomer/PC/Organoclay (20/75/5)		
H <sup>+</sup> SPS	3.36	26.3
Li <sup>+</sup> SPS	2.81	31.4
Na <sup>+</sup> SPS	2.72	32.5
K <sup>+</sup> SPS	*	*
Rb <sup>+</sup> SPS	*	*
Zn <sup>2+</sup> SPS	*	*
Zn <sup>2+</sup> SPS Ionomer/PC/Organoclay		
0/95/5	3.51	25.1
5/90/5	2.84	31.2
10/85/5	2.67	33.2
15/80/5	*	*
20/75/5	*	*

\*Exfoliated.

in the ionomer/PC blend showed a disappearance of the clay peak, indicating better dispersion of organoclay layers in the polymer matrix. This may be due to the ionic interactions between the ionic part of SPS and organoclay surface.

Figure 2 compares WAXD pattern of PC/SPS ionomer/organoclay nanocomposites with various cations (Li<sup>+</sup>, Na<sup>+</sup>, K<sup>+</sup>, Rb<sup>+</sup> and Zn<sup>2+</sup>) of the SPS ionomer. Only the SPS ionomer/PC/organoclay nanocomposites with smaller cations gave the intercalated structures. Smaller cation of the ionomers, Li<sup>+</sup> and Na<sup>+</sup>, resulted in intercalated structures, while bigger the cations such as K<sup>+</sup>, Rb<sup>+</sup> and Zn<sup>2+</sup> showed a disappearance of the peak due to the well dispersion of organoclay in the PC matrix, indicating a delaminated and disordered structure of the organoclay in the nanocomposites, even at 20 wt% of the ionomer loadings. These results clearly indicated that the extent of intercalation/exfoliation gradually increased with increasing cation size of ionomer. However, as described in the forthcoming paragraph cover-

ing TEM results, PC/SPS ionomer/organoclay nanocomposites prepared with  $K^+$  and  $Rb^+$  cations of SPS ionomer show both exfoliated and intercalated structures, but the extent of intercalation/exfoliation and distance between clay galleries gradually increased with increasing cation size of compatibilized ionomer. Figure 3 shows the WAXD pattern of  $Zn^{2+}$ SPS ionomer/PC/organoclay nanocomposites with various ionomer loadings ranging from 0 to 20 wt%. The results indicate that the lower ionomer loadings such as 5 and 10 wt% only showed intercalated structures with d-spacing of 31.2 and 33.2 Å, respectively. Nanocomposites with 15 wt% and above ionomer loadings reveal that the clay layers are delaminated and better dispersed in the polymer matrix. These results helped in understanding the optimum ionomer loading required to obtain the well-dispersed clay structures.

Figure 4 shows the TEM images of PC/SPS ionomer/organoclay nanocomposites compatibilizing with various cation of SPS ionomers. The structure of the clay in the nanocomposite was discussed above with the help of WAXD and these results are further confirmed by TEM analysis. Nanocomposites compatibilized with  $K^+$ ,  $Rb^+$  and  $Zn^{2+}$  ionomers exhibit better clay dispersion than those compatibilized with  $Li^+$  and  $Na^+$  ionomers. Sodium ionomer compatibilized nanocomposites (Figure 4(a)) shows parallel lines in the micrograph indicating that the clay layers were intercalated. Nanometer range intercalated clay tactoids are clearly shown in Figure 4(b), (c). Dark lines corresponds to the cross section of a clay sheet of ca. 1 nm thick and the gap between two adjacent lines is the inter layer spacing or gallery spacing. Figure 4(b) shows the micrograph of  $K^+$  iono-

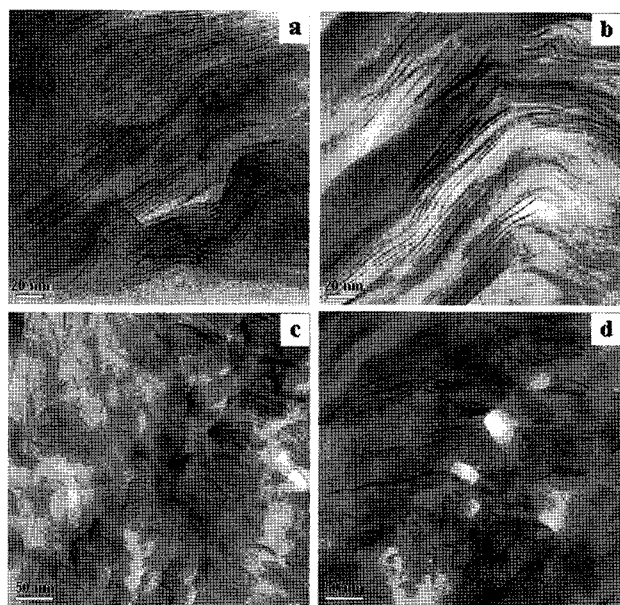


**Figure 4.** TEM images of PC/SPS ionomer/organoclay nanocomposite compatibilized with various ionomer cations of SPS (20 wt%): (a)  $Na^+$ , (b)  $K^+$ , (c)  $Rb^+$ , and (d)  $Zn^{2+}$ .

mer compatibilized nanocomposite reveal the partial exfoliation of clay platelets with mostly intercalated tactoids. Figure 4(c) shows the micrograph of  $Rb^+$  ionomer compatibilized nanocomposites resulting in the coexistence of the disordered, exfoliated platelets of clay layers and intercalated tactoids. However, the exfoliation/intercalation levels were gradually increased by increasing the cation size of ionomer from  $Na^+$  to  $Zn^{2+}$ . TEM micrograph of  $Zn^{2+}$  ionomer compatibilized nanocomposites presented in Figure 4(d) indicates that the clay layers were comparatively much better dispersed in the polymer matrix.

Preparation of PC/SPS ionomer/organoclay nanocomposites was explored by using SPS ionomers as compatibilizers during solution intercalation. Higher ionomer loading in the PC matrix led to better interactions with the modified clay layers resulting in a better dispersion. Bigger cations of the SPS ionomer such as  $K^+$ ,  $Rb^+$  and  $Zn^{2+}$  showed better interaction than the smaller cations such as  $Li^+$  and  $Na^+$ ; however, smaller cations showed only intercalated structures, while bigger cations showed well dispersed and disordered clay layers in the polymer matrix. This type of behavior was also observed by previous researches in nanocomposites prepared from ionomers of ethylene/methacrylic acid copolymers<sup>19</sup> and sulfonated sPS.<sup>22</sup> Exfoliated or intercalated organoclay structures can be obtained by adding 15 wt% of  $Zn^{2+}$ SPS ionomer as a compatibilizer in the polymer matrix. Ionomer of a bigger cation with higher radii and polarizability can enhance the interactions with the polar clay surface. Miscibility is also favored by increasing the concentration of the interacting functional group. Effect of ionomer cation size on dispersion of clay layers can also be explained by ion exchange process between the organoclay and ionomers. Few quaternary ammonium ions of organoclay can be exchanged by metal cations of the ionomers. The smaller cation of the ionomer is capable of entering the montmorillonite lattice structure by an irreversible exchange process due to its smaller size and higher reactivity, resulting in only intercalated structures. Thus, in the case of nanocomposites prepared from bigger cations of the ionomer, there are lower possibility for cation exchange reaction between the polymer and the organoclay, which results in a better dispersion of clay layers by ionic interaction.<sup>19</sup>

Melt crystallization behavior of PC/SPS ionomer blends and PC/SPS ionomer/organoclay nanocomposites were studied by DSC. Enthalpy of fusion ( $\Delta H$ ) for melting endotherm of PC/SPS ionomer blends and PC/SPS ionomer/organoclay nanocomposites after annealing for 15 h with 3 h intervals at 190 °C were measured and results were listed in Table II. PC/SPS ionomer blends with  $Li^+$  and  $Na^+$  cations did not crystallize even after annealing for 15 h at 190 °C. Blends with  $K^+$ ,  $Rb^+$  and  $Zn^{2+}$  were crystallized after a longer annealing time of 9 h and showed a melting endotherm. Nanocomposites with  $K^+$ ,  $Rb^+$  and  $Zn^{2+}$  were crystallized even at shorter annealing time (3 h) and showed a melting endot-

**Table II. DSC Crystallization Data of PC/SPS Ionomers (80/20) Blends with Various Ionomer Cations after Annealed at 190 °C**

Annealed Time (h)	$\Delta H$ (J/g)							
	Without Clay				With Clay			
	Na <sup>+</sup>	K <sup>+</sup>	Rb <sup>+</sup>	Zn <sup>2+</sup>	Na <sup>+</sup>	K <sup>+</sup>	Rb <sup>+</sup>	Zn <sup>2+</sup>
3	-no-	-no-	-no-	-no-	-no-	5.54	5.32	5.43
6	-no-	-no-	-no-	0.45	-no-	5.65	4.83	5.52
9	-no-	0.34	-no-	0.83	-no-	5.43	4.62	5.61
12	-no-	0.83	0.32	4.06	0.58	5.01	5.43	5.60
15	-no-	1.76	2.63	7.55	2.54	5.73	5.16	5.65

<sup>-no-</sup>Do not crystallized after annealing.

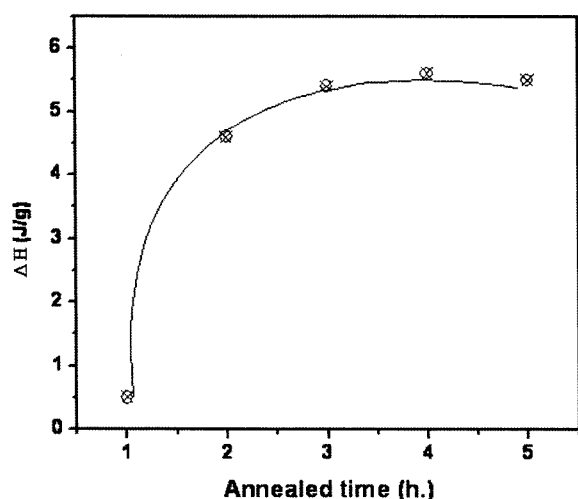


**Figure 5.** DSC endothermic plot of PC/Zn<sup>2+</sup>SPS ionomer (20 wt%)/organoclay nanocomposite after annealed at 190 °C for various time.

herm. However, PC/SPS ionomer/organoclay nanocomposites showed enhanced crystallization process than PC/SPS ionomer blends.

Figure 5 presents the DSC endotherm plot of nanocomposites prepared from Zn<sup>2+</sup>SPS ionomer (20 wt%)/PC blend, which exhibited a major endotherm peak at about 235 °C after annealing at 190 °C for 5 h with 1 h intervals. The enthalpy of fusion increased with an increase in annealing time as crystallization proceeded. In this study, we observed a maximum crystallization rate at 190 °C for SPS ionomer/PC blends and its nanocomposites. The melt crystallization process of organoclay dispersed PC/Zn<sup>2+</sup>SPS ionomer was completed in the first 3 h. The crystallization rate of the SPS ionomer/PC blend was enhanced with an incorporation of organoclay layers in the polymer matrix. Figure 6 compares DSC melting endotherm of PC nanocomposites compatibilized with various cations of SPS ionomer after being annealed at 190 °C for 3 h. No melting endotherm was observed for Li<sup>+</sup> and Na<sup>+</sup> cations annealed for 3 h, whereas

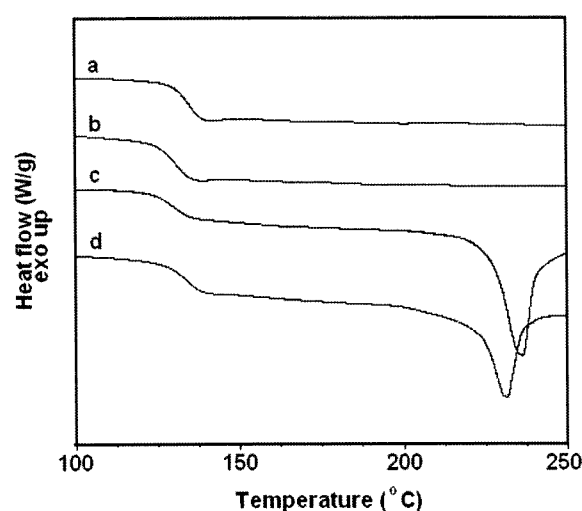


**Figure 6.** DSC melting thermogram of PC/SPS ionomer/organoclay nanocomposites compatibilized with various cations of SPS (20 wt%): (a) Li<sup>+</sup>, (b) Na<sup>+</sup>, (c) K<sup>+</sup>, and (d) Zn<sup>2+</sup> after annealed at 190 °C for 3 h.

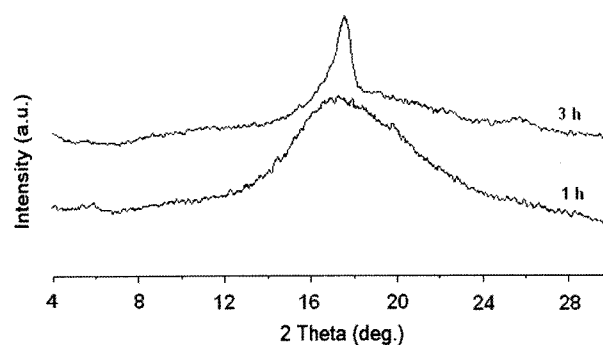


**Figure 7.** XRD pattern of PC/ Zn<sup>2+</sup>SPS ionomer (20 wt%)/organoclay nanocomposite after annealed at 190 °C for 1 and 3 h.

K<sup>+</sup> and Zn<sup>2+</sup> cations show well defined melting endotherm. Results are indicating that a well-dispersed organically modified clay can nucleate and enhance the crystallization of PC. These crystallization results were further confirmed by WAXD analysis. Figure 7 shows the WAXD pattern for

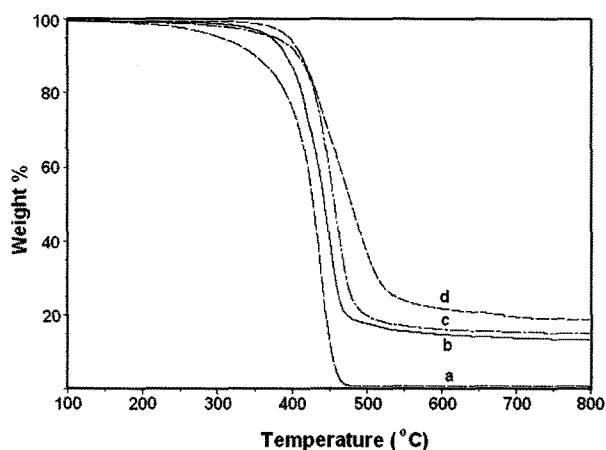


**Figure 8.** TGA thermogram of (a) SPS 3.0 mole%, (b) Zn<sup>2+</sup>SPS ionomer/PC (20/80) blend, (c) PC/ Zn<sup>2+</sup>SPS ionomer (20 wt%) blend/organoclay nanocomposite, and (d) pure PC.

PC/SPS ionomer/organoclay nanocomposite compatibilized with Zn<sup>2+</sup> cation of SPS ionomer after being annealed at 190 °C for 3 h with 1 h interval. The nanocomposite annealed at 190 °C for 1 h showed only a diffused amorphous pattern, which indicates that no crystallization occurred. After annealing for 3 h at 190 °C, a stronger and sharper peak at  $2\theta=17.69^\circ$  with d-spacing of 5.03 Å and a small peak at  $2\theta=25.70^\circ$  with d-spacing of 3.46 Å confirmed the crystallization of PC, which is consistent with results reported by Weiss *et al.*<sup>33</sup> for PC/Zn<sup>2+</sup>SPS blends.

The results indicate that well dispersed organoclay layers in the polymer matrix can enhance the crystallization process of PC/SPS ionomer blend. The nanocomposites prepared from K<sup>+</sup> and Zn<sup>2+</sup> cations of ionomer/PC blend showed better crystallization than the intercalated nanocomposites prepared from Li<sup>+</sup> and Na<sup>+</sup> cations. It seems that organoclay itself does not enhance the crystallization of PC in the absence of certain ionomer compatibilizers. Organoclay can enhance the crystallization of PC only in the presence of SPS ionomer compatibilizers with a variety of cations such as K<sup>+</sup>, Rb<sup>+</sup> and Zn<sup>2+</sup>. Similar results were reported by previous researchers for the PC nanocomposites in the presence of supercritical CO<sub>2</sub>.<sup>34</sup>

The thermal decomposition behavior evaluated by thermogravimetric analysis is shown in Figure 8. The Zn<sup>2+</sup>SPS/PC (20/80) blend shows an onset of decomposition at 400 °C, while Zn<sup>2+</sup>SPS/PC/organoclay shows an onset decomposition at 420 °C; these nanocomposites display delayed decomposition behavior compared to the Zn<sup>2+</sup>SPS ionomer/PC blend. The nano-dispersed lamellae of the clay in the polymer matrix may change the decomposition process of the polymer, since nano-dispersed silicate layers hinder the thermal transfer in the polymer matrix. It was observed that, organoclay layers enhanced the thermal stability of SPS ionomer/PC blends.

## Conclusions

PC/SPS ionomer/organoclay nanocomposites with exfoliated and intercalated clay structures can be prepared by compatibilizing with various cations of SPS ionomer. The dispersion of organoclay in the polymer matrix was improved by adding SPS ionomers as a compatibilizer. The efficiency of intercalation/exfoliation was improved by increasing the cation size and loading of SPS ionomer in the nanocomposite. Melt crystallization behavior of PC were dependent on the extent of clay dispersion in the ionomer compatibilized polymer matrix. Organoclay enhanced the crystallization of PC in the presence of SPS ionomers in the nanocomposites compared to that of the PC/SPS ionomer simple blend. Well-dispersed nanocomposites showed a better crystallization rate than the intercalated ones due to a nucleation effect of well dispersed nanolayers in the polymer matrix. Nanocomposites compatibilized with SPS ionomers showed better thermal stability than the PC/SPS ionomer blend because the nano-dispersed silicate layers hinder the decomposition process of matrix polymers, resulting in a delayed thermal decomposition.

**Acknowledgements.** This work was financially supported by the Korea Science and Engineering Foundation (KOSEF) grant funded by the Korea government (MOST) (Nos. R11-2007-050-02001-0 and R01-2007-000-10353-0). This work was supported by Nano R&D program through the Korea Science and Engineering Foundation funded by the Ministry of Education, Science and Technology (2008-02380). This work was also supported by the Seoul Research and Business Development Program (10816).

## References

- (1) P. C. LeBaron, G. Wang, and T. J. Pinnavaia, *Appl. Clay Sci.*, **15**, 11 (1999).
- (2) M. Alexander and P. Dubois, *Mater. Sci. Eng.*, **28**, 1 (2000).
- (3) S. S. Ray and M. Okamoto, *Prog. Polym. Sci.*, **28**, 1539 (2003).
- (4) E. Manias, *Nature Materials*, **6**, 9 (2007).
- (5) R. A. Vaia and E. P. Giannelis, *MRS Bull.*, **26**, 394 (2001).
- (6) Y. H. Kim, K. T. Bang, S. J. Choi, J. M. Kim, M. S. Han, and W. N. Kim, *Macromol. Res.*, **15**, 676 (2007).
- (7) J. C. Kim and J. H. Chang, *Macromol. Res.*, **15**, 449 (2007).
- (8) A. Kellarakis, E. P. Giannelis, and K. Yoon, *Polymer*, **48**, 7567 (2007).
- (9) B. Vonfalka and W. Rellensman, *Makromol. Chem.*, **75**, 122 (1965).
- (10) J. P. Mercier, G. Groeninckx, and M. Lesns, *J. Polym. Sci. Part C*, **16**, 2059 (1967).
- (11) L. Xu and R. A. Weiss, *Macromolecules*, **36**, 9075 (2003).
- (12) X. Hu and A. J. Lesser, *Polymer*, **45**, 2333 (2004).
- (13) X. B. Hu and A. J. Lesser, *J. Polym. Sci. Part B: Polym. Phys.*, **41**, 2275 (2003).
- (14) T. M. Wu and C. S. Liao, *Macromol. Chem. Phys.*, **201**, 2820

- (2000).
- (15) P. J. Yoon, D. L. Hunter, and D. R. Paul, *Polymer*, **44**, 5323 (2003).
- (16) X. Huang, S. Lewis, W. J. Brittain, and R. A. Vaia, *Macromolecules*, **33**, 2000 (2000).
- (17) N. N. Bhiwankar and R. A. Weiss, *Polymer*, **46**, 7246 (2005).
- (18) L. Cui and R. D. Paul, *Polymer*, **48**, 1632 (2007).
- (19) R. K. Shah and R. D. Poul, *Macromolecules*, **39**, 3327 (2006).
- (20) C. I. Park, O. O. Park, J. G. Lim, and H. J. Kim, *Polymer*, **42**, 7465 (2001).
- (21) C. I. Park, W. M. Choi, M. H. Kim, and O. O. Park, *J. Polym. Sci. Part B: Polym. Phys.*, **42**, 1685 (2004).
- (22) P. Govindaiah, S. R. Mallikarjuna, and C. Ramesh, *Macromolecules*, **39**, 7199 (2006).
- (23) G. D. Barber, B. H. Calhoun, and R. B. Moore, *Polymer*, **46**, 6706 (2005).
- (24) B. J. Chisholm, R. B. Moore, G. Barber, F. Khouri, A. Hempstead, M. Larsen, E. Olson, J. Kelley, G. Balch, and J. Caragher, *Macromolecules*, **35**, 5508 (2002).
- (25) Z. M. Wang, H. Nakajima, E. Manias, and T. C. Chung, *Macromolecules*, **36**, 8919 (2003).
- (26) J. A. Lee, M. Kontopoulou, and J. S. Parent, *Polymer*, **46**, 5040 (2005).
- (27) S. Subramani, S. W. Choi, J. Y. Lee, and J. H. Kim, *Polymer*, **48**, 4691 (2007).
- (28) J. A. Lee, M. Kontopoulou, and J. S. Parent, *Macromol. Rapid Commun.*, **28**, 210 (2007).
- (29) Y. H. Shin, W. D. Lee, and S. S. Im, *Macromol. Res.*, **15**, 662 (2007).
- (30) X. Lu and R. A. Weiss, *Macromolecules*, **29**, 1216 (1996).
- (31) R. Xie and R. A. Weiss, *Polymer*, **39**, 2851 (1998).
- (32) X. Lu and R. A. Weiss, *Macromolecules*, **24**, 4381 (1991).
- (33) X. Lu and R. A. Weiss, *Macromolecules*, **25**, 6185 (1992).
- (34) T. K. Kwei, Y. K. Dai, X. Lu, and R. A. Weiss, *Macromolecules*, **26**, 6583 (1993).
- (35) R. A. Weiss, L. Shao, and R. D. Lundberg, *Macromolecules*, **25**, 6370 (1992).
- (36) M. Hara and A. Eisenberg, *Macromolecules*, **17**, 1335 (1984).
- (37) M. Hara and A. Eisenberg, *Macromolecules*, **20**, 2160 (1987).
- (38) Z. Gao, A. Molnar, F. M. Morin, and A. Eisenberg, *Macromolecules*, **25**, 6460 (1992).
- (39) R. Tannenbaum, M. Rutkowska, and A. Eisenberg, *J. Polym. Sci. Part B: Polym. Phys.*, **25**, 663 (1987).
- (40) D. H. Kim and S. C. Kim, *Macromol. Res.*, **16**, 457 (2008).
- (41) R. A. Weiss and X. Lu, *Polymer*, **35**, 1963 (1994).
- (42) F. Kucera and J. Jancar, *Chem. Papers*, **50**, 224 (1996).